Y. Basheer et al., "Active power control of a hybrid power plant comprising hydropower, battery and supercapacitor to provide frequency control," 9th Hybrid Power Plants & Systems Workshop (HYB 2025), Hybrid Conference, Åland Islands, Finland, 2025, pp. 34-41, doi: 10.1049/icp.2025.2368.

ACTIVE POWER CONTROL OF A HYBRID POWER PLANT COMPRISING HYDROPOWER, BATTERY AND SUPERCAPACITOR TO PROVIDE FREQUENCY CONTROL

Yasir Basheer[1], Juan I. Pérez-Díaz[*1], Marcos Blanco[2], Jesús Fraile-Ardanuy[1], Jorge Nájera[2], Gustavo Navarro[2], José Ignacio Sarasúa[1]

[1] Universidad Politécnica de Madrid, Madrid, Spain
[2] Unidad de Accionamientos Eléctricos, CIEMAT, Madrid, Spain

[*]ji.perez@upm.es

Keywords: HYBRID POWER PLANT, HYDROPOWER, BATTERY, SUPERCAPACITOR, FREQUENCY CONTROL

Abstract

Energy storage systems are integral to modern power systems for integrating renewable energy sources. This study focuses on a hybrid energy storage system integrated into a hydro power plant. The hybrid system comprises a battery and supercapacitor and cooperates with the hydropower plant in providing primary and secondary frequency control through an ad hoc control system. The control system has two main objectives. On the one hand, it distributes the frequency control effort between the hydropower units, the battery and the supercapacitor, and on the other hand, tries to keep the state of charge (SOC) of the battery and supercapacitors within pre-specified bounds. When the SOC of the energy storage units reaches the predefined upper or lower bounds, the hydro power plant intervenes to restore the SOC to within such bounds. Two symmetrical SOC bands around a central SOC value are defined for each, the battery and supercapacitor, for this purpose. The main goal of this paper is the definition of the SOC control bands and central value to reduce battery aging and wear and tear on different components of the hydro power plant, while providing a quality frequency control action. Specifically, the strategy addresses reducing penstock stress, limiting the distance travelled by the wicket gates, and minimizing the direction changes in the wicket gate movement. Simulation models of the hydro power plant, battery, and supercapacitor were developed to validate the proposed control system. The results highlight the effectiveness of the strategy in achieving acceptable frequency control performance goals while reducing wear and tear on both the energy storage components and the hydro power plant infrastructure.

1. Introduction

With ongoing changes brought into power system architectures, largely driven by the swift expansion of intermittent wind and solar renewable energy sources (RESs) [1], significant challenges and opportunities have presented themselves. Traditionally, hydropower provides grid regulation services. Now, it has also to be involved in supporting the variation brought about by RES integration. This shift puts more demand on the capacity of hydropower plants (HPPs) to respond efficiently and fairly frequently, which in turn puts a certain polarization between the plants in their operations and mechanical know-how [2, 3]. Hence, one of the focus areas is how HPPs can further increase the flexibility and responsiveness of their active power regulating systems without leading to accelerated wear of equipment. While the optimization of the current configuration of HPPs remains of high interest, novel solution approaches are also being pursued for increased operational flexibility. One, of course, is the joint use of hydropower with battery energy storage, so-called hydro battery regulation concept, which was investigated through the European XFLEX Hydro initiative [4]. In parallel, the Hydro WIRES program of the U.S. Department of Energy is investigating, with a focus on fast-response energy storage such as batteries, generation-side storage solutions to support run-of-river (ROR) HPPs [5]. Similarly, the German utility RWE is engaged in a project for the integration of large-scale battery energy storage systems (ESSs) with ROR-HPPs [6].

Batteries may certainly act as support to hydropower for the provision certain ancillary services. However, specific, especially in regions where said technological integration is currently rare, which is why more studies are to be conducted yet. In the future, it is likely that HPPs will take precedence as an instrument for grid regulation rather than merely supplying energy. Frequency control is one of the main ancillary services provided by HPPs, directly affecting grid stability and revenue from plant operations [3]. Frequency control is generally assessed in terms of stability and responsiveness, with stability being of utmost importance. It is during these times that challenges arise, triggered by negative damping effects from governor actions and water hammer effects into the process of ultra-low frequency oscillations (ULFOs), especially in systems with high hydropower penetration [7]– [9].

As regards primary frequency control (PFC), highly sensitive governor settings are applied by several HPPs. However, this

might increase the possibility of ULFOs, thus emphasizing the contradictions between fast response and system stability. A wide range of studies have been carried out that aim to find a solution to this dilemma. For instance, numerous control schemes and adjustments to governor parameters are suggested to raise regulation quality [10], [11]. Others have resorted to multi-objective optimizations and novel control approaches to alleviate this negative damping while preserving the responsiveness of PFC [12]– [14].

A frequency limitation controller (FLC) might be practical in some situations, such as HPPs situated at high-voltage direct current (HVDC) transmission endpoints [15], [16]. However, this solution is difficult to apply to traditional alternating current (AC) grids because it is specific to DC systems. This highlights even more the need for cutting-edge, broadly applicable solutions that improve flexibility. A viable way to enhance grid services is by integrating fast-response ESSs with the current hydropower infrastructure, particularly large-capacity units. The possibility of strengthening frequency regulation by combining HPPs with flywheels [18], [19], and supercapacitors [20], [21] has been investigated in previous studies. Research on battery-hydropower hybrid systems is still lacking, though, especially when it comes to how well they work together in frequency control situations. Although joint operation in power regulation mode has been studied in some studies [22], they frequently ignore dynamic behaviors that are essential for PFC and secondary frequency control (SFC).

A model predictive control strategy was proposed to reduce penstock stress, but it did not take battery sizing into account [23]. Other methods simplify hydraulic dynamics by modeling them as ramp limits [24]. Overall, rather than evaluating how such hybridization changes the fundamental dynamics of hydropower systems, most of the previous research has concentrated on control-level enhancements. Furthermore, rather than implementation on the generating (or unit) side, several studies focus on the coordination at the grid or system level [25]– [27].

Driven by the increase in the penetration of renewable sources, the focus on energy storage systems and technologies has been further accentuated [28–30]. Various storage techniques abound, such as batteries, supercapacitors, flywheels, and compressed air. Each of these storage options exhibits diverse technical characteristics, particularly in terms of power and energy response characteristics. To compensate for the deficiencies of single storage technologies, thereby improving overall efficiency and reducing degradation, hybrid energy storage systems (HESS) have been suggested [31-33]. Such storage systems are hybrids of two energy storage technologies, which normally involve the combination of storage technologies with a high energy density and another one with a high-power density, e.g. batteries with supercapacitors. In places where power demand changes aggressively, supercapacitors immediately respond because of their high-power density and ability to discharge quickly. As power demand starts to level off, batteries gradually take over to ensure sustained and steady power delivery [34–36]. Besides, this strategic sharing of power between the energy storage devices enhances the life span of HESS and cuts down energy and material losses [37–39].

This paper focuses on the coordinated operation of a hydropower plant with a HESS comprising a battery ESS (BESS) and a supercapacitor ESS (SCESS). The coordinated operation is meant to provide both PFC and SFC with the highest possible quality and to reduce the wear in different components of the hydropower plant and the aging of the battery.

The main contributions of this paper are twofold:

1. To analyze how different control strategies and control system settings influence the penstock stress, wear in the turbine regulating mechanism, battery ageing and control signal tracking error.

2. To investigate the dynamic behavior and interaction of the supercapacitor with the hydropower units and batteries, in a hybrid configuration.

2. Methodology

In order to pursue the above-mentioned objectives, a dynamic simulation model has been developed using Matlab-Simuink. Figure 1 shows an upper-level block diagram of the model. As can be seen in the figure, the simulation model uses as input a frequency signal. The simulation comprises submodels of the automatic generation control system, the hydropower plant, the battery and the supercapacitor. In addition, there's a central block by which the coordinated control of the hybrid power plant is realized.

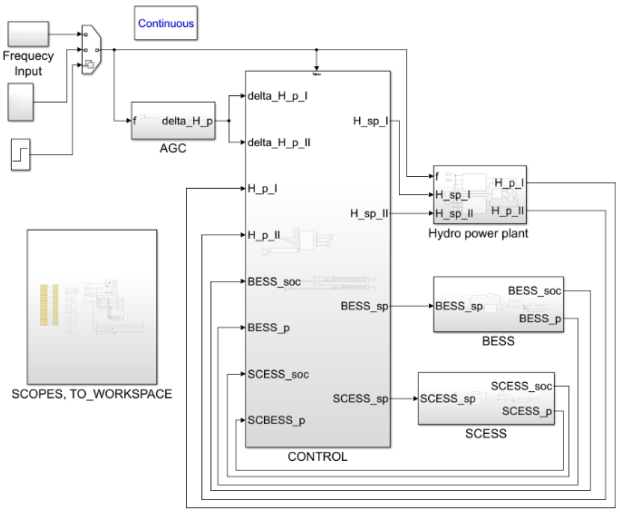

Figure 1. Upper-level block diagram of the simulation model.

2.1 AGC model

The AGC model emulates the performance of the TSO's centralized control system, aimed to generate an SFC set-point for each regulation zone providing SFC as a function of the system's area control error, and the company's control system, aimed to distribute the SFC set-point between the online units providing SFC. The latter task can be modulated through a specific parameter (named *aFRR* in the results section). The AGC model is based on the one used in [40]. The k-factor and time constants used in the AGC model are consistent with the

currently in force regulations and common practice in the Spanish power system.

2.2 Hydropower plant model

The dynamic model of the hydropower plant is composed of the conduits, the turbines, and their respective governors, see Figure 2. The model receives as inputs the system frequency (f) and the control signal for each unit (H_sp_I and H_sp_II). These signals determine the changes in the electric power that the plant delivers to the system at each moment, H_p_I and H_p_II.

To model the penstock shared by both units, the lumped parameter method has been used in order to incorporate the pipe's elasticity and the fluid's compressibility into the model [41]. Given the short length of this conduit, a single segment has been used. For the same reason, the sections connecting the penstock to each unit and the discharge conduits have been neglected. The water level in both the upper reservoir, hu_0, and the discharge area, hd_0, remain constant throughout the simulations.

The turbines have been modelled according to the guidelines in [42]. It has been assumed that the dynamic response of the electrical machines is instantaneous, so that the electrical power is always equal to the mechanical power. A conventional proportional-integral (PI) controller has been implemented in each turbine governor. The dynamics of the wicket gates movement have been introduced into the model through a first-order transfer function. Similarly, the opening and closing speed of the wicket gates has been limited in accordance with [42].

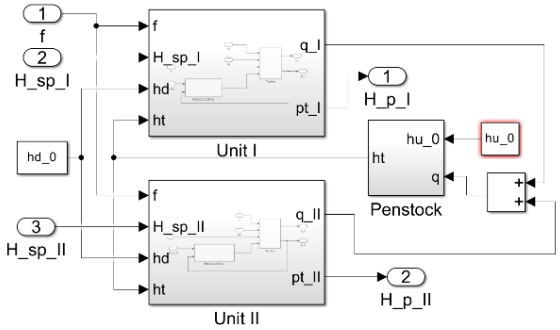

Figure 2. Hydropower plant block diagram.

2.3 Energy storage system models

There are several ways to model Li-ion BESS and SCESS, and for this work a semi-empirical approach has been followed. This approach allows for having mathematical models that imitate the dynamic behavior of the devices using electric circuit elements such as resistors, inductors and capacitors. These models use ordinary differential equations, which reduce the computational effort and facilitate implementation with respect to other model architectures such as electrochemical models. The models of both the BESS and the SCESS are developed in MATLAB Simulink. It is important to note that the parameters of both the BESS and SCESS models have been calibrated from various experimental tests.

2.3.1 BESS model

The BESS model is adapted from the work presented in [43], and builds upon the classical Shepherd model, which relates voltage, current, internal resistance, and SoC.

The main difference from the standard Shepherd model, as depicted in Fig. 3, is the representation of internal resistance. In this version, it is split into two components: ohmic resistance and polarization resistance. This distinction modifies the voltage/runtime behaviour of the BESS system.

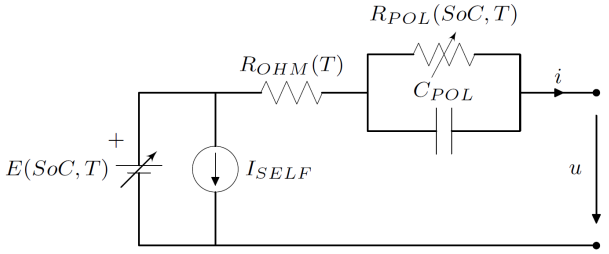

Figure 3. BESS model scheme.

The thermal model consists of two parts: heat generation and heat dissipation. Introducing thermal effects causes the voltage/runtime parameters to vary with temperature. Heat generation accounts for three contributions: ohmic losses, irreversible heat, and reversible heat. Heat evacuation is simplified by assuming only surface-to-ambient transfer.

Aging in the BESS model includes both calendar and cycling degradation. Cycling aging depends on temperature, C-rate, and Ah throughput, while calendar aging is influenced by SoC, temperature, and storage time.

More detailed explanations are available in [43].

2.3.2 SCESS model

The SCESS model builds upon the formulation introduced in [44], introducing key adaptations to account for the frequency-dependent behavior of two SC cells connected in series, along with their balancing circuitry. This structure enables straightforward scaling to larger stacks of series-connected cells. The model diagram is depicted in Fig. 4, where the model parameters vary as a function of the SoC.

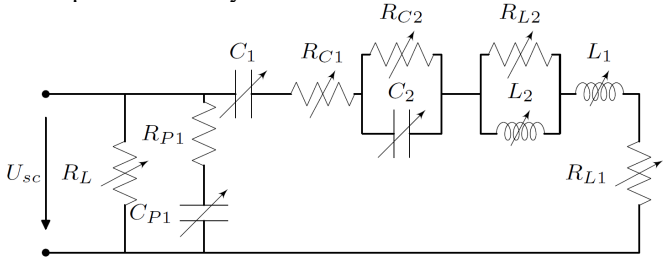

Figure 4. SCESS model scheme.

The thermal behaviour of the SC is addressed using a similar methodology to that applied in the Li-BESS model. It includes a heat generation model, comprising both reversible and irreversible heat sources, and a heat transfer model that assumes energy exchange between the cell surface and the ambient environment.

Further details can be found in [44].

2.4 Control system

Figure 5 shows the block diagram of the hybrid plant's control system. As can be seen in the figure, the hybrid plant's control system has 2 main objectives:

- Distribute the frequency control effort between the hydropower units, the BESS and the SCESS.
- Keep the SOC of the BESS and SCESS within pre-specified bounds (band sizes) through a coordinated effort of the hydropower units.

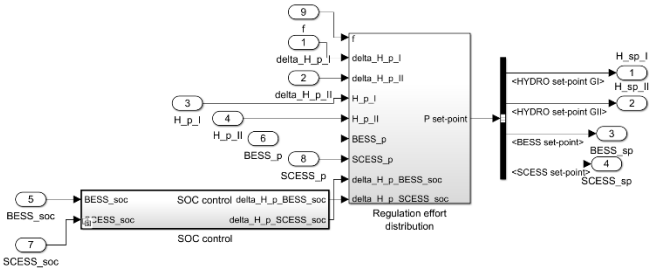

Figure 5. Hybrid plant's control system.

The hybrid plant's control system is based on the one presented in [45]. The control loop aimed to distribute the control effort between the hydropower units, the BESS and the SCESS is based on a series of low-pass filters aimed to split the frequency control effort into slow, intermediate and fast components. These components are then sent, respectively, to the hydropower units, the BESS and the SCESS. The control loop aimed to control the SOC of the BESS and the SCESS is based on a series of relays aimed to activate/deactivate the participation of the hydropower units in the SOC control when the SOC of the BESS or SCESS goes out of/in an outer/inner band centred around a 50-% SOC. Two different band sizes have been used in the results section, 5 % and 20 %, according to Figure 6.

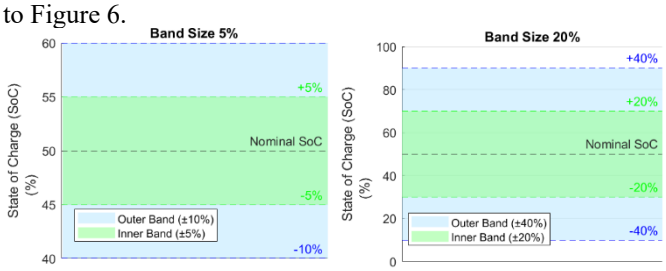

Figure 6. Band sizes considered in the SOC control loop.

3. Results

The simulation model described in previous section has been used to simulate operation of the hybrid power plant assuming different plant configurations, control settings and frequency scenarios. 10 representative frequency profiles have been obtained from a set of historical frequency time series of the UK power system. The simulations have been performed assuming 3 different plant configurations (config=1/2/3 – hydropower only/hydropower+battery/hydropower+battery+supercapacitor), 2 different "intensities" of participation in the SFC (aFRR=0/1 – only PFC/PFC+moderate participation in the SFC), and 2 different band sizes (BS=5%/20. The results of the simulations are summarized in this section.

Figures 7-9 are aimed to present a general overview of the performance of the hydropower plant when it operates in stand-alone mode and when it operates in a coordinated manner with the BESS and SCESS. Figure 7 shows the response of the hydropower plant in the lower graph under the frequency control set-points that can be seen in the intermediate graph. These set-points are a consequence of the frequency shown in the upper graph. The participation of the hydropower plant in the SFC is moderate in the figure, i.e. aFRR=1.

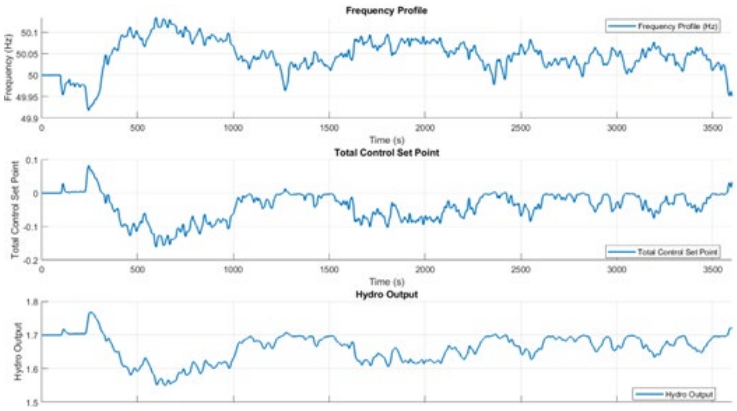

Figure 7: Hydropower plant response (config=0, aFRR=1).

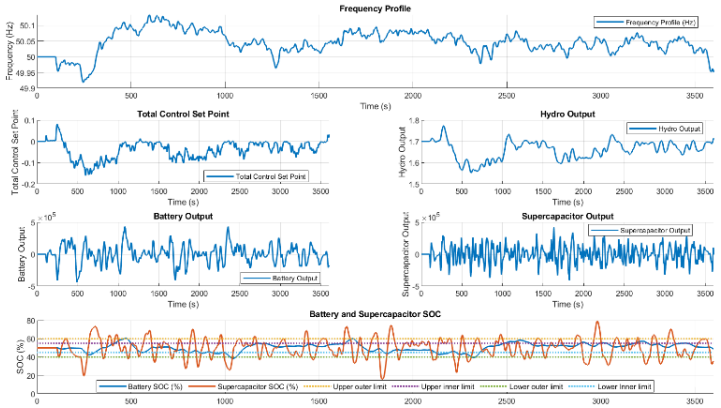

Figure 8: Hybrid power plant response (config=0, aFRR=1, BS=5%).

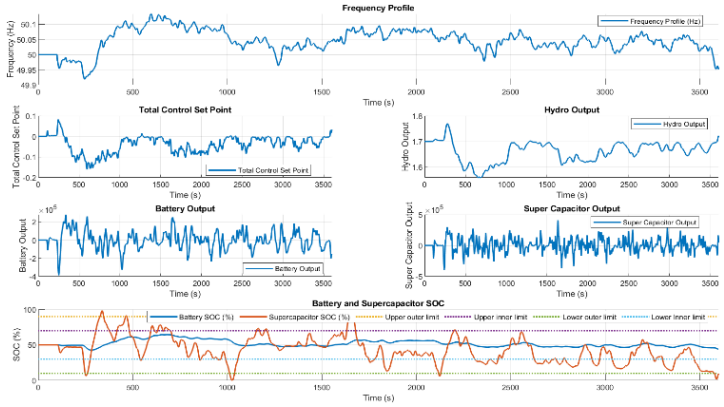

Figure 9: Hybrid power plant response (config=0, aFRR=1, BS=20%).

Figure 8 and 9 show in turn the response of the hybrid power plant under the same frequency profile and with the same aFRR as Figure 7, when the SOC control loop uses a band size of 5 % and 20 %, respectively. By comparing these 2 figures with Figure 7, one can easily see how the hydropower plant

output is smoothed thanks to the coordinated operation with the BESS and the SCESS. Additionally, from Figures 8 and 9 one can also see how often the SOC of the SCESS goes out of the outer band of the SOC control loop with the considered band sizes. A smoother hydropower plant output should in principle result in a lower tear in the regulating mechanism of the turbine. However, we'd like to pay attention also to other operational parameters, namely: penstock stress, battery ageing and control signal tracking error.

The results below are organized as follows: first, several figures showing the impact of the coordinated operation with the BESS (config=2) are presented, and then, a table is included summarizing how much such an impact changes when the SCESS is added (config=3).

Figure 10 demonstrates that the BESS contributes in all analysed cases to reduce the penstock stress, both when the hybrid power plant provides only PFC and when it provides both PFC and SFC, with the two considered band sizes. The reduction in the penstock stress is higher with a band size of 20 %.

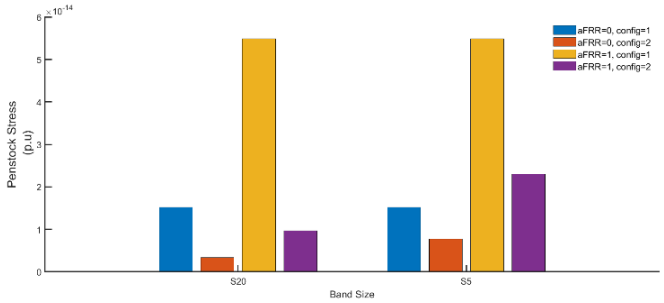

Figure 10: Effect of the BESS in the penstock stress.

The wear in the turbine regulating system is analysed in Figure 11 as a function of the total distance travelled by the wicket gates. As can be seen the figure, the BESS contributes to slightly reduce the wear in the turbine regulating mechanism only with the higher band size. With the smaller band size, the total distance travelled by the wicket gates increases in the coordinated operation with the BESS. As expected, the total distance travelled by the wicket gates increases when the hybrid power plant provides both PFC and SFC.

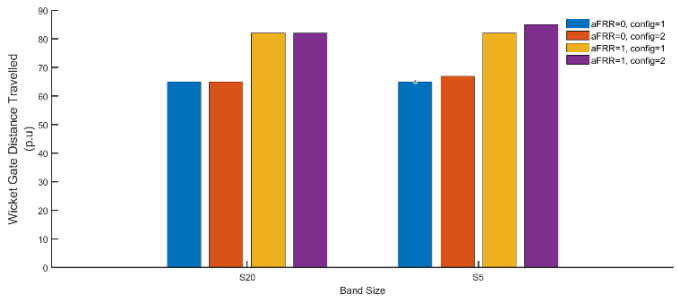

Figure 11. Total distance travelled by the wicket gates.

Figure 12 shows another metric reflecting the wear in the turbine regulating mechanism: the number of direction changes in the wicket gate movement. As can be seen in the Figure, this metric also benefits from the coordination with the BESS. However, the effect of the band size is not systematic.

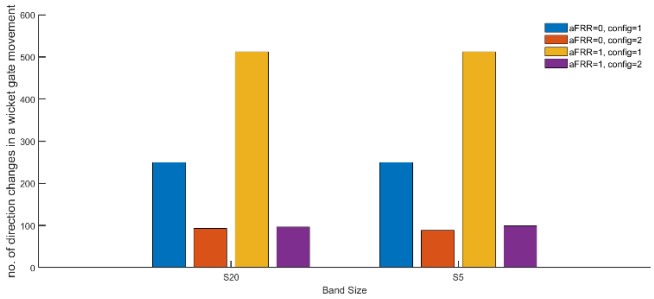

Figure 12. Number of direction changes in the wicket gate movement.

The battery benefits significantly from wider bands, as can be seen in Figure 13. As expected, the battery ageing increases when the hybrid power plant provides both PFC and SFC.

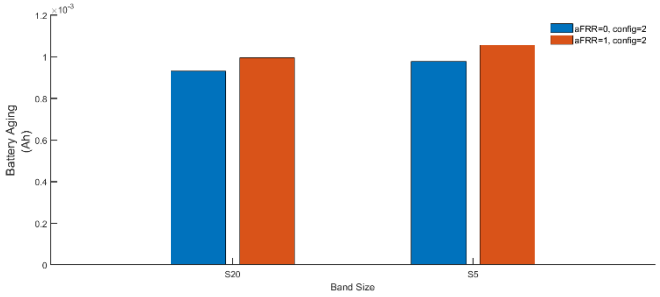

Figure 13. Battery ageing.

Finally, the metric that most benefits from the coordinated operation with a BESS is with no doubt the control signal tracking error. As can be seen in Figure 14, it decreases significantly thanks to the coordinated operation with the BESS. The reduction is slightly greater with a band size of 20 %.

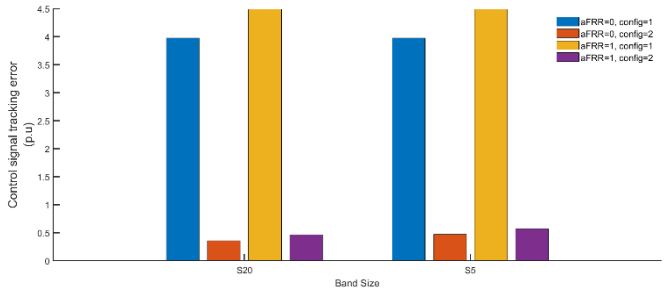

Figure 14. Control signal tracking error.

The effects resulting from the coordination with the BESS and the SCESS are summarized in Table I. Identifying systematic effects (across all values of aFRR and band sizes) of the SCESS on the considered metrics is not straightforward, e.g. the penstock stress increases with the SCESS when a band size of 20 % is used, but does not show a systematic trend when a band size of 5 % is used. An analogous comment may be made as regards the effect of the SCESS on the turbine regulating

mechanism: no systematic effect can be identified from the results included in the table.

An evident advantage of incorporating the SCESS is the overall reduction in the battery aging across all values of aFRR and band sizes. The SCESS reduces the depth and frequency of battery charge-discharge cycles by taking over of part of the frequency control effort. . As shown in Table I, this effect is consistent but becomes more pronounced with a wider SOC control band. Another evident advantage of adding the SCESS can be found in the control signal control signal tracking error. As can be seen in the Table I it is significantly lower with the SCESS. This may have important implications for the system's stability and could be leveraged through fast frequency control ancillary services.

Table I. Compared results of Adding Supercapacitor on band sizes

Band Size 5%								
aFRR	**config**	**Penstock stress (p.u)**	**Direction Changes (no.)**	**Wicket Gate Distance (p.u)**	**Battery Aging (Ah)**	**Δ %**	**Control signal tracking error (p.u)**	**Δ %**
0	2	7.72157E-15	89	67	0.000979		0.468681873	
0	3	1.90011E-14	99	67	0.0008629	11.86	0.005284618	98.87
1	2	2.30056E-14	99	85	0.0010558		0.572882449	
1	3	2.26048E-14	97	85	0.0009183	13.02	0.005837589	98.98
Band Size 20%								
0	2	3.33464E-15	93	65	0.0009326		0.358060688	
0	3	5.44672E-15	93	65	0.0007995	14.27	0.003843025	98.93
1	2	9.68872E-15	97	82	0.0009955		0.461460089	
1	3	1.80341E-14	99	83	0.0008296	16.66	0.076999474	83.31

4. Conclusion

This paper studies the coordinated operation of a hybrid power plant comprising a hydropower plant, a battery, and a supercapacitor. The performance of the hybrid power plant is analysed by means of simulations under different plant configurations, control settings and "intensities" of the plant's participation in the secondary frequency control.

As can be seen from the results, the battery contributes to reduce the penstock stress, the wear in the turbine regulating mechanism and the control signal tracking error. In general, the magnitude of these effects is higher with a wider band size in the SOC control loop.

The incorporation of a supercapacitor may contribute to further reduce the penstock stress and the wear in the turbine regulating mechanism under certain circumstances, and helps significantly reduce the battery ageing and, particularly, the control signal tracking error.

Further work is required to study the optimal sizing of the battery and the supercapacitor from a multiobjective perspective, and to explore other control strategies.

5 Acknowledgements

This his work has been funded by MICIU/AEI/10.13039/501100011033/UniónEuropeaNextGenerationEU/PRTR through Project TED2021-132794B-C21 and Project TED2021-132794A-C22. In addition, the authors would like to thank NATURGY for sharing with them design and operational data of the hydropower plant.

6 References

[1] Q. Guo, F. Xiao, C. M. Tu, F. Jiang, R. W. Zhu, J. Ye, and J. Y. Gao, "An overview of series-connected power electronic converter with function extension strategies in the context of high-penetration of power electronics and renewables," Renewable and Sustainable Energy Reviews, vol. 156, pp. 111934, Mar. 2022.

[2] W. J. Yang, P. Norrlund, L. Saarinen, A. Witt, B. Smith, J. D. Yang, and U. Lundin, "Burden on hydropower units for short-term balancing of renewable power systems," Nature Communications, vol. 9, no. 1, pp. 2633, Jul. 2018.

[3] J. P. Hoffstaedt, D. P. K. Truijen, J. Fahlbeck, L. H. A. Gans, M. Qudaih, A. J. Laguna, J. D. M. De Kooning, K. Stockman, H. Nilsson, P. T. Storli, B. Engel, M. Marence, and J. D. Bricker, "Low-head pumped hydro storage: a review of applicable technologies for design, grid integration, control and modelling," Renewable and Sustainable Energy Reviews, vol. 158, pp. 112119, Apr. 2022.

[4] D. Valentín, A. Presas, M. Egusquiza, J. L. Drommi, and C. Valero, "Benefits of battery hybridization in hydraulic turbines. Wear and tear evaluation in a Kaplan prototype," Renewable Energy, vol. 199, pp. 35– 43, Nov. 2022.

[5] HydroWIRES Initiative Research Roadmap. (2022). U.S. Department of Energy, America. [Online]. Available: https://www.energy.gov/sites/default/files/2022-02/HydroWIRES%20Roadmap%20FINAL%20%28508%20Compliant%29 0.pdf.

[6] WORLD-ENERGY. (2021, Aug.). RWE combines hydropower with mega-batteries to balance grid. [Online]. Available: https://www.worl d-energy.org/article/19733.html.

[7] X. D. Lu, C. S. Li, D. Liu, Z. W. Zhu, and X. Q. Tan, "Influence of water diversion system topologies and operation scenarios on the damping characteristics of hydropower units under ultra-low frequency oscillations," Energy, vol. 239, pp. 122679, Jan. 2022.

[8] W. J. Yang, P. Norrlund, J. Bladh, J. D. Yang, and U. Lundin, "Hydraulic damping mechanism of low frequency oscillations in power systems: quantitative analysis using a nonlinear model of hydropower plants," Applied Energy, vol. 212, pp. 1138–1152, Feb. 2018.

[9] J. J. Zhang, A. Mahmud, W. Govaerts, D. Y. Chen, B. B. Xu, and H. L. Xiong, "Sensitivity analysis and low frequency oscillations for bifurcation scenarios in a hydraulic generating system," Renewable Energy, vol. 162, pp. 334–344, Dec. 2020.

[10] L. Saarinen, P. Norrlund, W. J. Yang, and U. Lundin, "Allocation of frequency control reserves and its impact on wear and tear on a hydropower fleet," IEEE Transactions on Power Systems, vol. 33, no. 1, pp. 430–439, Jan. 2018.

[11] L. M. Chen, X. Lu, Y. Min, Y. W. Zhang, Q. Chen, Y. M. Zhao, and C. Ben, "Optimization of governor parameters to prevent frequency oscillations in power systems," IEEE Transactions on Power Systems, vol. 33, no. 4, pp. 4466–4474, Jul. 2018.

[12] Z. G. Zhao, J. D. Yang, Y. F. Huang, W. J. Yang, W. C. Ma, L. Y. Hou, and M. Chen, "Improvement of regulation quality for hydro-dominated power system: quantifying oscillation characteristic and multi-objective optimization," Renewable Energy, vol. 168, pp. 606–631, May 2021.

[13] G. Chen, F. Tang, H. B. Shi, R. Yu, G. H. Wang, L. J. Ding, B. S. Liu, and X. N. Lu, "Optimization strategy of hydrogovernors for eliminating ultralow-frequency oscillations in hydrodominant power systems," IEEE Journal of Emerging and Selected Topics in Power Electronics, vol. 6, no. 3, pp. 1086–1094, Sep. 2018.

[14] N. Kishor, R. P. Saini, and S. P. Singh, "A review on hydropower plant models and control," Renewable and Sustainable Energy Reviews, vol. 11, no. 5, pp. 776–796, Jun. 2007.

[15] W. J. Yang, Y. F. Huang, Z. G. Zhao, J. D. Yang, and J. B. Yang, "Stability region of hydropower plant with surge tank at HVDC sending terminal," Energy Science & Engineering, vol. 9, no. 5, pp. 694–709, May 2021.

[16] W. C. Wu, X. R. Wang, and X. Xiao, "Multiple DC coordinated suppression method for ultra-low frequency oscillations," Sustainable Energy Technologies and Assessments, vol. 53, pp. 102301, Oct. 2022.

[17] J. I. Perez-D ´ ´ıaz, M. Lafoz, and F. Burke, "Integration of fast acting energy storage systems in existing pumped-storage power plants to enhance the system's frequency control," WIREs Energy and Environment, vol. 9, no. 2, pp. e367, Mar./Apr.. 2020.

[18] C. L. Jin, N. Lu, S. Lu, Y. Makarov, and R. A. Dougal, "Coordinated control algorithm for hybrid energy storage systems," in 2011 IEEE Power and Energy Society General Meeting, 2011, pp. 1–7.

[19] C. L. Jin, N. Lu, S. Lu, Y. V. Makarov, and R. A. Dougal, "A coordinating algorithm for dispatching regulation services between slow and fast power regulating resources," IEEE Transactions on Smart Grid, vol. 5, no. 2, pp. 1043–1050, Mar. 2014.

[20] V. Gevorgian, E. Muljadi, Y. S. Luo, M. Mohanpurkar, R. Hovsapian, and V. Koritarov, "Supercapacitor to provide ancillary services," in 2017 IEEE Energy Conversion Congress and Exposition (ECCE), 2017, pp. 1030–1036.

[21] J. Kim, V. Gevorgian, Y. S. Luo, M. Mohanpurkar, V. Koritarov, R. Hovsapian, and E. Muljadi, "Supercapacitor to provide ancillary services with control coordination," IEEE Transactions on Industry Applications, vol. 55, no. 5, pp. 5119–5127, Sep./Oct. 2019.

[22] T. Makinen, A. Leinonen, and M. Ovaskainen, "Modelling and benefits ¨ of combined operation of hydropower unit and battery energy storage system on grid primary frequency control," in 2020 IEEE International Conference on Environment and Electrical Engineering and 2020 IEEE Industrial and Commercial Power Systems Europe (EEEIC / I&CPS Europe), 2020, pp. 1–6.

[23] S. Cassano and F. Sossan, "Model predictive control for a medium-head hydropower plant hybridized with battery energy storage to reduce penstock fatigue," Electric Power Systems Research, vol. 213, pp. 108545, Dec. 2022.

[24] A. Schreider and R. Bucher, "An auspicious combination: fast-ramping battery energy storage and high-capacity pumped hydro," Energy Procedia, vol. 155, pp. 156–164, Nov. 2018.

[25] T. Ma, H. X. Yang, and L. Lu, "Feasibility study and economic analysis of pumped hydro storage and battery

storage for a renewable energy powered island," Energy Conversion and Management, vol. 79, pp. 387– 397, Mar. 2014.

[26] M. S. Javed, D. Zhong, T. Ma, A. T. Song, and S. Ahmed, "Hybrid pumped hydro and battery storage for renewable energy based power supply system," Applied Energy, vol. 257, pp. 114026, Jan. 2020.

[27] M. Guezgouz, J. Jurasz, B. Bekkouche, T. Ma, M. S. Javed, and A. Kies, "Optimal hybrid pumped hydro-battery storage scheme for offgrid renewable energy systems," Energy Conversion and Management, vol. 199, pp. 112046, Nov. 2019.

[28] Lawder, M.T.; Suthar, B.; Northrop, P.W.C.; De, S.; Hoff, C.M.; Leitermann, O.; Crow, M.L.; Santhanagopalan, S.; Subramanian, V.R. Battery Energy Storage System (BESS) and Battery Management System (BMS) for Grid-Scale Applications. Proc. IEEE 2014, 102, 1014–1030. [Google Scholar] [CrossRef]

[29] Hou, H.; Chen, Y.; Liu, P.; Xie, C.; Huang, L.; Zhang, R.; Zhang, Q. Multisource Energy Storage System Optimal Dispatch Among Electricity Hydrogen and Heat Networks From the Energy Storage Operator Prospect. IEEE Trans. Ind. Appl. 2021, 58, 2825–2835. [Google Scholar] [CrossRef]

[30] Abomazid, A.M.; El-Taweel, N.A.; Farag, H.E.Z. Optimal Energy Management of Hydrogen Energy Facility Using Integrated Battery Energy Storage and Solar Photovoltaic Systems. IEEE Trans. Sustain. Energy 2022, 13, 1457–1468. [Google Scholar] [CrossRef]

[31] Guo, S.; Kurban, A.; He, Y.; Wu, F.; Pei, H.; Song, G. Multi-Objective Sizing of Solar-Wind-Hydro Hybrid Power System with Doubled Energy Storages Under Optimal Coordinated Operational Strategy. CSEE J. Power Energy Syst. 2022, 9, 2144–2155. [Google Scholar]

[32] Li, X.; Ma, R.; Yan, N.; Wang, S.; Hui, D. RResearch on Optimal Scheduling Method of Hybrid Energy Storage System Considering Health State of Echelon-Use Lithium-Ion Battery. IEEE Trans. Appl. Supercond. 2021, 31, 0604204. [Google Scholar] [CrossRef]

[33] Naderi, E.; Bibek, K.C.; Ansari, M.; Asrari, A. Experimental Validation of a Hybrid Storage Framework to Cope With Fluctuating Power of Hybrid Renewable Energy-Based Systems. IEEE Trans. Energy Convers. 2021, 36, 1991–2001. [Google Scholar] [CrossRef]

[34] Zhang, X.; Feng, G. MMC-Based PV Grid-Connected System With SMES-Battery Hybrid Energy Storage System. IEEE Trans. Appl. Supercond. 2024, 34, 5702004. [Google Scholar] [CrossRef]

[35] Liu, Y.; Li, P.; Xing, Z.; Han, X.; Fu, Q.; Jiang, Z. Research on Microgrid Superconductivity-Battery Energy Storage Control Strategy Based on Adaptive Dynamic Programming. IEEE Trans. Appl. Supercond. 2024, 34, 5701604. [Google Scholar] [CrossRef]

[36] Xie, Q.; Bin Zhao, R.; Tang, M.G.; Hu, S.Y.; Xu, H.Y.; Tan, X.S.; Yang, L. A DC Voltage Sag Compensator Based on SMES-Battery Hybrid Energy Storage. IEEE Trans. Appl. Supercond. 2021, 31, 5701005. [Google Scholar] [CrossRef]

[37] Zhou, S.; Chen, Z.; Huang, D.; Lin, T. Model Prediction and Rule Based Energy Management Strategy for a Plug-in Hybrid Electric Vehicle With Hybrid Energy Storage System. IEEE Trans. Power Electron. 2020, 36, 5926–5940. [Google Scholar] [CrossRef]

[38] Rasool, S.; Muttaqi, K.M.; Sutanto, D. A Multi-Filter Based Dynamic Power Sharing Control for a Hybrid Energy Storage System Integrated to a Wave Energy Converter for Output Power Smoothing. IEEE Trans. Sustain. Energy 2022, 13, 1693–1706. [Google Scholar] [CrossRef]

[39] Yan, N.; Zhang, B.; Li, W.; Ma, S. Hybrid Energy Storage Capacity Allocation Method for Active Distribution Network Considering Demand Side Response. IEEE Trans. Appl. Supercond. 2018, 29, 5700204. [Google Scholar] [CrossRef]

[40] Pérez-Díaz, J. I.; Sarasúa, J. I.; Wilhelmi, J. R. Contribution of a hydraulic short-circuit pumped-storage power plant to the load–frequency regulation of an isolated power system. International Journal of Electrical Power & Energy Systems. 2014, 62, 199-211.

[41] Kishor, N.; Saini, R. P.; Singh, S. P. A review on hydropower plant models and control. Renewable and Sustainable Energy Reviews. 2007, 11(5), 776-796.

[42] Mover, W. G. P.; Supply, E. Hydraulic turbine and turbine control models for system dynamic studies. IEEE Transactions on Power Systems. 1992, 7(1), 167-179.

[43] Nájera, J.; Arribas, J. R.; De Castro, R. M.; Núñez, C. S. Semi-empirical ageing model for LFP and NMC Li-ion battery chemistries. Journal of Energy Storage. 2023, 72, 108016.

[44] Navarro Soriano, G. (2022). Modelado y dimensionado de un sistema de almacenamiento basado en supercondensadores para la integración en red de energías renovables (Doctoral dissertation, Industriales).

[45] Casarin, S.; Cavazzini, G.; Pérez-Díaz, J. I. Battery and Flywheel hybridization of a reversible Pumped-Storage Hydro Power Plant for wear and tear reduction. Journal of Energy Storage. 2023, 71, 108059.